DAMAGING DOWNSLOPE WIND EVENTS IN THE SAN GABRIEL VALLEY OF SOUTHERN CALIFORNIA

SCOTT SUKUP
NOAA/NWS, Oxnard, California

1. Introduction

The complex terrain of southern California (Fig. 1) poses a number of forecast challenges for various types of wind events that impact the region. For example, there are the well documented “sundowner” winds along the Santa Ynez Range of Santa Barbara County (Ryan 1996). There are also the infamous and heavily researched Santa Ana winds that can fuel large wildfires throughout much of southern California (Raphael 2003). Another type of wind event that is less well-known is the “Palmdale Wave”, which affects the Antelope Valley in Los Angeles (LA) County (Fig. 2), and is associated with strong south or southwest flow over the San Gabriel Mountains (Kaplan and Thompson 2005). The San Gabriel Mountains (SGM) also play an important role in damaging northerly wind events that impact the San Gabriel Valley (SGV) and eastern portions of the San Fernando Valley (SFV) (Fig. 2). Like the “Palmdale Wave”, there is little research on this last type of wind event and thus it is the focus of this paper.

The motivation for this paper largely comes from an extreme northerly wind event that brought widespread damage across much of the SGV and eastern portions of the SFV from the late evening hours on 30 November 2011 through the early morning hours on 1 December 2011 (Fig. 3). Some of the highlights of this event include: 13 Proclamations of Local Emergency; 350,000 residents in the SGV losing power, some for over a week; an estimated $40 million in damages; a ground-stop and multiple power outages at Los Angeles International Airport (LAX) that resulted in 23 flights being diverted to Ontario International Airport (ONT).

Another motivating factor for this study was that damaging wind events in the SGV can be difficult to predict for a number of reasons. One reason is that damaging northerly wind events, such as the 1 December 2011 event, are very rare. Another reason is that Santa Ana events, which are associated with NE to ENE winds for parts of LA County, typically produce very little wind in the SGV; however, the synoptic-scale conditions can be similar to northerly wind events such as the 1 December 2011 event. The complex terrain of LA County and relatively coarse resolution of numerical models commonly used in operations, such as the 12-km North American Mesoscale Model (NAM), can also make forecasting wind events in the SGV difficult, as these models cannot fully resolve the winds in the boundary layer, let alone forecast small-scale details such as mountain waves and downslope wind storms.

The last motivating factor for this study is the fact that the SGV is a densely populated area with over 2 million residents, thus damaging wind events can be highly impactful, as was the case on 1 December 2011. Therefore, the main goal of this study was to gain a better understanding of the synoptic and mesoscale conditions that can produce damaging winds in the SGV. In the following section, mountain waves and downslope wind storms will be discussed and the geography of LA County will be examined closer. Next, a 35-year climatology of damaging wind events in the SGV will be presented. This will be followed by several case studies, including a more detailed analysis of the 1 December 2011 event.

2. Mountain Waves, Downslope Wind Storms, and Geography

Mountain wave systems can occasionally produce downslope windstorms (Durran and Klemp 1983). For mountain waves to form above and downstream of a topographic barrier, there are two basic requirements in the upstream environment: 1) a significant component of the vector wind should be perpendicular to the ridgeline and 2) the environment should be stable (COMET® Program 2014). For the first requirement, Durran (1990) stated that the prevailing winds should be within 30° of perpendicular of the ridgeline. With regards to the second requirement, the atmosphere is stable under normal atmospheric conditions, so prevailing winds perpendicular to the ridgeline are sufficient for mountain wave development under most circumstances. In addition to the above requirements for mountain wave development, strong downslope winds that reach the surface on the lee side of a mountain range are usually associated with a temperature inversion near the ridgetop (Durran and Klemp 1983).

The SGM are about 5000-8000 ft tall, with some of the peaks in eastern LA County as high as 10,000 ft (Fig. 2). As seen in Figure 2, the SGM are oriented roughly east-west, such that a meteorological wind direction of about 10° across the Antelope Valley would be perpendicular to the ridgeline and thus ideal for mountain waves or downslope winds to impact the SGV and eastern portions of the SFV (orange shaded region in Figure 2).

Santa Ana winds, which are out of the NE or ENE, normally result in little or no wind for the SGV and LA Coastal Plain. Instead, Santa Ana winds typically funnel through the lower mountain ranges in western LA County and continue down through the Santa Clarita Valley and the valleys of Ventura County. The western portions of the SFV and the Santa Monica Mountains often experience gusty winds during Santa Ana events as well. Although damaging winds in the foothill and valley areas immediately south of the SGM are very rare with Santa Ana events, it should be noted that mountain wave activity and downslope winds would be possible with a meteorological wind direction as northeasterly as 40°, according to the 30° rule stated by Durran (1990).

During strong NW wind events, damaging winds can occur through the Interstate 5 Corridor and down through the Santa Clarita Valley. Occasionally damaging winds reach the northern SFV during NW wind events, but almost never reach the SGV. So, it can be seen that unique conditions are required for damaging winds to occur in the SGV, as it is often sheltered from the more common NW and NE wind events. The rarity of such events will be demonstrated in the climatology that follows.

3. Climatology

a) Data and Methodology

To put the 1 December 2011 event into a historical perspective and identify additional events to study and compare to the 1 December 2011 event, a 35-year climatology of similar events was created using a qualitative approach. To do this, the National Climatic Data Center (NCDC) Storm Data publications were reviewed from 1979-1996 and the NCDC Online Storm Events Database was reviewed from 1996-2014. Starting with the 1979-1980 winter season, the months of October through March were reviewed, as these are the months when strong upper-level troughs tend to bring high wind events to southern California. For these dates, the storm summaries were simply searched for mention of wind damage in cities and communities roughly within the orange shaded region in Figure 2 that were associated with north to NE wind events. From this point forward please note that when the terms "wind damage" or "damaging winds" are used, it refers to the orange shaded region in Figure 2 unless otherwise specified.

b) Climatology Results

Using the above methodology, eight events were identified from the NCDC storm summaries between 1979 and 2014. A ninth event that occurred on 6 January 2003 was identified through personal communication with David Bruno (Senior Forecaster at NWS Los Angeles/Oxnard), but was not initially found using the NCDC storm summaries. Wind damage for the 6 January 2003 event was documented online by The City of Rosemead (2014). The dates of the nine events are listed below in Table 1:

Damaging Wind Events (1979 – 2014)	
12 January 1985	6 January 1997*****
21 February 1985*****	6 January 2003*****
23 November 1986	30 December 2010
17 February 1988*****	1 December 2011*****
1 January 1996	

Table. 1. North to northeast wind events from October 1979 through March 2014 with documented damage in the foothill and valley communities south of the San Gabriel Mountains (roughly the orange shaded area in Figure 2). Events with an asterisk (*) are presented in the case studies section.

Qualitative review of the NCDC storm summaries revealed that there was only one other event of similar magnitude to 1 December 2011, which occurred on 6 January 1997. Much like the 1 December 2011 event, the 6 January 1997 event had significant widespread wind damage, with a Local State of Emergency declared in 11 cities (Fig. 4). The remaining seven events consisted of wind damage that was less widespread in nature (Fig. 5). Unlike the 1 December 2011 and 6 January 1997 events, there was no mention of any Local State of Emergencies in the NCDC storm summaries for the seven remaining events. Figure 5 also shows that the foothill and valley areas immediately to the south of the SGM in the extreme eastern portion of the SFV, seems to be an area more likely to experience damaging wind events. This includes cities such as La Crescenta-Montrose and La Cañada Flintridge. Seven of the nine events had damaging winds documented in this area. Meanwhile, damaging winds in the central and eastern portion of the SGV were less common. In addition to the 1 December 2011 and 6 January 1997 events, only the 17 February 1988 and 6 January 2003 events had wind damage documented in this area. In all, it appears that damaging wind events associated with north to NNE flow over the SGM occur about once every 3-5 years, while extreme widespread events such as 1 December 2011 may only occur about once every 10-20 years.

The main caveat of the climatology is that the findings are subject to the detail of the NCDC storm summaries. Many of the storm summaries prior to the mid-1990s are not as descriptive as those from more recent years, so it is possible that some of the less extreme events were missed during the earlier years. However, it seems likely that the 1 December 2011 and 6 January 1997 events were the two most extreme events during the 35-year period from 1979 to 2014, and certainly for the 20-year period starting around the mid-1990s. In the following section, the 1 December 2011 event and four other events (indicated in Table 1) are presented.

4. Case Studies

a) Data and Methodology

In this section, five events that produced damaging winds are presented and synoptic-scale conditions are compared. The synoptic-scale features that are compared for each event include the 500 mb and MSLP patterns, surface pressure gradients, the presence of a near-ridgetop temperature inversion, upper-level winds, and the strength of the synoptic-scale subsidence associated with cold air advection (CAA). The cases presented here attempt to demonstrate the synoptic-scale differences between the extreme events like 1 December 2011 and other damaging, but less severe events.

The North American Regional Reanalysis (NARR) is used to show the 500 mb and MSLP patterns at the approximate start time of each event. The strength of the observed surface pressure gradients are assessed using MSLP differences between several Automated Surface Observing System (ASOS) sites. The strength of the northerly pressure gradient is examined using MSLP differences between Los Angeles International Airport (LAX) and San Francisco International Airport (SFO), along with LAX and Bakersfield (BFL). The northeasterly pressure gradient is evaluated using MSLP differences between LAX and Daggett (DAG). LAX-SFO, LAX-BFL, and LAX-DAG are all values that are commonly used by forecasters at NWS Los Angeles/Oxnard (LOX) to help them predict the strength of wind events. LAX-DAG is often used to assess the strength of Santa Ana events. The locations of LAX, SFO, BFL and DAG are shown in Figure 1. The presence of a near-ridgetop temperature inversion is examined using soundings from Vandenberg Air Force Base (VBG) and Desert Rock (DRA). The locations of VBG and DRA are also shown in Figure 1.

The upper-level winds and the synoptic-scale subsidence associated with CAA are also examined using the NARR. Both are evaluated for a grid point over the SGM at 700 mb. The synoptic-scale subsidence due to CAA is assessed by calculating the temperature advection term of the quasi-geostrophic (QG) omega equation. This is Term B on the right hand side of equation 5.6.11 from Bluestein (1992). The calculations are made using Unidata's General Meteorology Package (GEMPAK) in a manner similar to that described by Galarneau (2014).

In addition to the above data sources, Remote Automated Weather Station (RAWS) observations and short-range forecasts from the 12-km NAM are used to evaluate some of the mesoscale features associated with the 1 December 2011 event.

b) The 1 December 2011 event

Figure 6 provides a synoptic overview of the event that brought widespread damaging winds on 1 December 2011. At 0600 UTC 30 November 2011 the 500 mb trough that would eventually cause the damaging winds, was entering the Pacific Northwest (Fig. 6a). Over the next 24 hours the trough aggressively dug southward with a 552 dam closed low starting to develop at 500 mb over southern Nevada by 0600 UTC 1 December 2011 (Fig. 6b-c), setting up strong northerly flow at mid-levels over much of California. This was also around the time when the damaging winds in the foothill and valley areas south of the SGM began. Meanwhile at the surface, a 1040 mb high was building into British Columbia at 1800 UTC 30 November 2011 (Fig. 6b). By 0600 UTC 1 December 2011, the surface high had strengthened to 1044 mb and became oriented roughly east-west, setting up a strong north-south surface pressure gradient across southern California (Fig. 6c). Eventually the upper-level trough became a fully developed cutoff low centered over southeastern California on the morning of 1 December 2011 (Fig. 6d).

Strong winds in the mountains of northwestern LA County began after 0000 UTC 1 December 2011, following the passage of a strong cold front. The 97 mph gust in the mountains of northwestern

LA County shown in Figure 3 was measured by the Whitaker Peak RAWS around 0300 UTC 1 December 2011 at an elevation of about 4100 ft. Figure 7 shows the general north-south progression of the cold front and timing of the damaging winds across the lower elevations. The Saugus RAWS indicated the cold front passing through the Santa Clarita Valley around 2300 UTC 30 November 2011, as the winds shifted from SSW to NNW (Fig. 7a). Winds then shifted to the north and NNW at Van Nuys (VNY) and Burbank (BUR) around 0100 UTC 1 December 2011 (Fig. 7b-c), as the cold front swept through the SFV. By 0300 UTC 1 December 2011 the cold front had pushed through the SGV, with NNE winds beginning to increase at the Santa Fe Dam around 0600 UTC 1 December 2011 (Fig. 7d).

While strong winds out of the NNE continued across the mountains well into the evening hours on 1 December 2011, it is important to note that the damaging winds across the foothill and valley areas adjacent to the SGM were short-lived in comparison. All reports of damaging winds in the foothill and valley communities in the eastern part of the SFV and western portion of the SGV occurred about 0600-0900 UTC 1 December 2011, while damaging winds further east in the central and eastern SGV occurred approximately 0900-1200 UTC 1 December 2011. This is supported by the observations at BUR and the Santa Fe Dam. At BUR, a brief period of strong winds occurred around 0700 UTC 1 December 2011, as NNE winds gusted to about 55 mph (Fig. 7c). At the Santa Fe Dam, damaging winds occurred from about 1000-1200 UTC 1 December 2011, with NNE winds gusting 60-65 mph (Fig. 7d). Some of the harder hit locations in the western portion of the SGV, such as Pasadena, may have experienced as many as 3-4 hours of damaging winds according to trained weather spotters, but most locations only observed 1-2 hours of damaging winds. The relatively short-lived and shifting nature of the damaging winds is evidence that downslope winds with breaking waves aloft were involved, as this is a common characteristic of mountain wave systems (COMET® Program 2014).

Isentropic analysis of the NAM forecast winds on the 291K potential temperature surface at 0600 UTC 1 December 2011 shows that prevailing winds across the Antelope Valley were near perpendicular to the SGM at 50-55 kt out of the NNE (Fig. 8). Over the ridge tops, NNE winds increased to 60-65 kt, with the 291K surface near 800 mb (Fig. 8). The 0000 UTC 1 December 2011 sounding from the Vandenberg Air Force Base (VBG), which was taken an hour or two following the passage of the cold front at this location, indicated a strong temperature inversion, also near 800 mb or about 6000 ft (red temperature profile in Fig. 9). Thus, in the environment upstream of the mountain range, winds were near perpendicular to the ridgeline and there was a temperature inversion near the ridge top; two essential ingredients for downslope wind storms.

The isentropic analysis also indicates a region of strong isentropic descent on the lee side of the mountains, with the 291K surface sloping from 800 mb across the ridge tops down to 860 mb across the valley areas adjacent to the mountains (Fig. 8). A cross-section through eastern LA County shows the isentropic descent as well, with downward sloping isentropes on the lee side of the mountains, along with some impressive omega values of 60-65 μbs^{-1} (Fig. 10). Another important feature to note in the cross-section (Fig. 10) is the low-level wind maxima of 55-60 kt over the Antelope Valley below about 800 mb, which was the height of the inversion. Winds above this level decreased to about 30 kt just above 700 mb. This highlights the importance of the direction and strength of the winds below the height of the inversion in the upstream environment.

As previously shown, damaging winds began several hours following the passage of the cold front. It was at this time when the synoptic-scale subsidence associated with the CAA was the strongest (Fig. 11b). Figure 11b also illustrates that the damaging winds began as the 700 mb winds shifted from the NW to the NNE and increased to 50 kt from 0300-0900 UTC 1 December 2011. Note that the 20 kt wind at 700 mb in the NARR at 0600 UTC 1 December 2011 (Fig. 11b) is likely bad data. The 700 mb winds over the SGM at this time were likely around 40-45 kt out of the NNE, as indicated in the NAM cross-section (Fig. 10). The timing of the damaging winds also coincided with the strongest northerly surface pressure gradients, with LAX-SFO reaching about -15 mb from 0600-1200 UTC 1 December 2011

(Fig. 11a). LAX-BFL during this time was -6 to -8 mb, while LAX-DAG was around 0 mb (Fig. 11a). The exceptionally strong northerly gradient values along with near neutral LAX-DAG values is a good indicator that this was a strong northerly wind event, rather than a typical Santa Ana event.

c) The 6 January 1997 event

The 6 January 1997 event is presented here because it was the only other northerly wind event in the 35-year climatology that was of comparable magnitude to the 1 December 2011 event in terms of wind damage. Much like the 1 December 2011 event, the 6 January 1997 event was associated with a positively tilted trough at 500 mb, with a closed low starting to develop near the southern tip of Nevada at the start time of the event (Fig. 12a-b). Eventually a fully developed cutoff low developed in the 6 January 1997 event as well (not shown). The MSLP pattern in the 6 January 1997 event was also similar, with a large east-west oriented surface high pressure system (Fig. 12a-b). The surface high was weaker in the 6 January 1997 case at about 1036 mb; however, the axis of the surface high was further south than the 1 December 2011 event, so there was still a strong north-south surface pressure gradient over southern California (Fig. 12a-b). The time series shows that the LAX-SFO gradient values were strong, but weaker than the 1 December 2011 event, at about -10 to -11 mb when the damaging winds occurred (Fig. 13a); however, LAX-BFL was between -6 and -8 mb at this time (Fig. 13a), which was about the same as the 1 December 2011 event.

There was a slight northeasterly component to the surface pressure gradients when the damaging winds occurred in the 6 January 1997 event, with LAX-DAG between -3 and -4 mb (Fig. 13a). The NARR also indicated that the 700mb winds at that time were slightly more northeasterly in the 6 January 1997 event (Fig. 13b) in comparison to the 1 December 2011 event. Although the 700 mb winds were more northeasterly from 1200-1800 UTC 6 January 1997, the meteorological wind direction was 20-30°, so downslope winds and mountain wave activity were still a possibility. The DRA sounding from 1200 UTC 6 January 1997 (green temperature profile in Fig. 9) indicated a temperature inversion near 700 mb, which also supports the possibility of downslope winds. The higher altitude of the inversion in the 6 January 1997 event may explain why this event appears to have had more substantial damage in the eastern portion of the SGV (Fig. 4) than the 1 December 2011 event (Fig. 3), as some of the higher ridgelines in the eastern SGM are near 700-750 mb or about 8,000-10,000 ft. In the 6 January 1997 event, four cities in the eastern SGV declared a Local State of Emergency (Fig. 4), whereas the worst damage in the 1 December 2011 event was concentrated in the western part of the SGV (Fig. 3).

Much like the 1 December 2011 event, the start time of the wind damage in the 6 January 1997 event coincided with the onset of the strong synoptic-scale subsidence associated with the CAA (Fig. 13b). It is also interesting to note that although the strong CAA continued through the day on 6 January 1997 and the 700 mb winds strengthened to 55-60 kt, the damaging winds occurred mostly before 1800 UTC 6 January 1997 (Fig. 13b). A slight weakening of the surface pressure gradients (Fig. 13b) and a small shift in the direction of the 700 mb winds from 20-30° to 30-40° may explain this; however, another contributor may have been a less stable atmosphere during the daytime. Whiteman and Whiteman (1974) found that there is a tendency for downslope wind storms to occur at night when the atmosphere is more stable.

d) The 21 February 1985 event

The 21 February 1985 event is discussed here, because although the 500 mb pattern was similar to the 1 December 2011 and 6 January 1997 events (Fig. 12a-c), the wind damage was much less severe. Documented wind damage with this event appears to have been more isolated (Fig. 5). Once again, there was a deep trough over the western U.S. with a closed low starting to develop at 500 mb near the southern tip of Nevada at the start time of the event (Fig. 12c). Like the previous two cases, this became a fully developed cutoff low (not shown). However, it can be seen that the MSLP pattern was much different in the 21 February 1985 event, as the surface high pressure system remained centered off the west coast (Fig. 12c). Figure 14a shows that the damaging winds with this event began as LAX-SFO reached about -10 mb, which was similar to the 6 January 1997 event. The damaging winds also began as the 700 mb winds turned to the north and NNE (Fig. 14b).

The 21 February 1985 event was likely less severe than the previous two events for several reasons, but mainly because the best upper-level support, CAA, and strongest north-south surface pressure gradients did not overlap. At about -4 mb, LAX-BFL was 2-4 mb weaker than the previous two cases when the damaging winds occurred, but it strengthened to -6 to -7 mb later on 21 February 1985 (Fig. 14a); however, the strongest synoptic-scale subsidence associated with the CAA was over by that time (Fig. 14b). Furthermore, the synoptic-scale subsidence associated with the CAA was weakening when the strongest winds at 700 mb occurred (Fig. 14b). Another factor may have been a weaker inversion. The VBG sounding from 0000 UTC 21 February 1985 did show a weak temperature inversion near 800 mb (black temperature profile in Figure 9), but it was not as sharp as it was during the 1 December 2011 event.

e) The 17 February 1988 event

The 17 February 1988 event is discussed here for several reasons. Although the 500 mb pattern at the start time of this event looked quite similar to the 1 December 2011 and 6 January 1997 events (Fig. 12a, b, d), the wind damage was more isolated once again (Fig. 5). Additionally, a closed low never developed at 500 mb like it did in the previous three cases, as the upper-level trough did not dig southward as aggressively (not shown). Instead, the 17 February 1988 event was associated with a faster moving 500 mb trough, that quickly progressed NW to SE across the Great Basin (not shown). It should be noted that the 12 January 1985, 23 November 1986, and 1 January 1996 events were associated with a similar upper-level pattern (not shown). Furthermore, the 17 February 1988 event was one of only four events with documented wind damage in the eastern portion of the SGV (Fig. 5).

At the surface, the MSLP pattern in the 17 February 1988 event looked very similar to the 6 January 1997 event at the start time of the damaging winds, both in the position and the orientation of the surface high pressure system (Fig. 12b, d). However, the surface high in the 17 February 1988 event was not as strong at 1028 mb, which resulted in a weaker north-south surface pressure gradient. The weaker north-south surface pressure gradient during this event can be seen in both LAX-SFO and LAX-BFL. When the damaging winds occurred, LAX-SFO was around -4 mb (Fig. 15a). This was less than half the value of LAX-SFO for the previous three cases examined here. Additionally, LAX-BFL was about -3 to -5 mb when the damaging winds occurred (Fig. 15a), compared to -6 to -8 mb in the 1 December 2011 and 6 January 1997 events.

Although the 17 February 1988 event had a weaker north-south surface pressure gradient than the 1 December 2011 and 6 January 1997 events, the upper-level support was similar. Figure 15b shows that north to NNE winds at 700 mb increased to 50 kt at the time of the event. The timing of the damaging winds also coincided with the onset of the strongest synoptic-scale subsidence associated with the CAA. While there were no DRA or VBG soundings available on the morning of 17 February 1988 when the damaging winds occurred, the DRA sounding from 0000 UTC 18 February 1988 did show a sharp temperature inversion around 800 mb (blue temperature profile in Figure 9). Thus, it appears that the weaker north-south surface pressure gradient was the main reason why the 17 February 1988 event was not as severe as the 1 December 2011 and 6 January 1997 events.

f) The 6 January 2003 event

The last event that will be covered here occurred on 6 January 2003. This event is presented to demonstrate that damaging winds in the SGV can occur when the MSLP pattern resembles that of a typical strong Santa Ana event. As seen in Figure 12e, a surface high pressure system was centered over the interior western U.S. at the start time of the event, setting up a strong northeasterly surface pressure gradient over southern California. What made this an atypical Santa Ana event was the closed low at 500 mb over NW Arizona, near the southern tip of Nevada (Fig. 12e). While there was some wind damage in the SGV and eastern portions of the SFV (Fig. 5), it is important to realize that this event was not as severe as the 1 December 2011 and 6 January 1997 events.

The time series of LAX-SFO, LAX-BFL, and LAX-DAG were much different than the previous cases. Most notably, LAX-DAG strengthened to -9 mb at the start time of the damaging winds (Fig. 16a), indicating that this was a very strong Santa Ana event. Strong Santa Ana events typically have a LAX-DAG value of about -8 mb or stronger. LAX-SFO and LAX-BFL on the other hand, were weakening throughout the event, although LAX-BFL was around -7 mb at the start time of the damaging winds (Fig. 16a).

The 1200 UTC 6 January 2003 sounding from DRA indicated two sharp temperature inversions. One near the ridgetop of the SGM at about 750 mb and another around 550 mb (purple temperature profile in Figure 9). The NARR data also indicates that the 700 mb winds were 40-50 kt out of the NNE (20-35°) on the morning of 6 January 2003 when the damaging winds occurred (Fig. 16b). Therefore, conditions allowed for the possibility of downslope winds and mountain wave activity. Also similar to most of the previous cases, was that the damaging winds began around the onset of the strongest synoptic-scale subsidence associated with the CAA (Fig. 16b). The 6 January 2003 event was not as severe as the 1 December 2011 and 6 January 1997 events, likely because it was a NE wind event, making it less favorable for mountain waves or downslope winds.

5. Summary and Conclusions

Damaging wind events in the SGV and eastern SFV that are associated with strong north to NNE flow over the SGM are a very rare phenomenon. From October 1979 through March 2014, there were only nine events with documented wind damage in this area. Of these nine events, the 1 December 2011 and 6 January 1997 events were the only events to produce widespread damage across most of the foothill and valley areas south of the SGM. It is estimated that extreme events such as these occur about once every 10-20 years, while less significant events occur once every 3-5 years.

The case studies presented here showed the synoptic-scale conditions that can produce wind damage in the foothill and valley areas south of the SGM. The case studies also attempted to identify the differences between the extreme events like 1 December 2011 and 6 January 1997, and some less extreme, but still damaging events. It was shown that the extreme events are more likely when the following synoptic-scale conditions overlap:

1) *Conditions are favorable for downslope winds.* This includes a temperature inversion near the ridgetops of the SGM (800-700 mb or 5,000-10,000 ft) and moderate to strong prevailing winds that are roughly perpendicular to the ridgeline. A meteorological wind direction of 10° is ideal.
2) *A deepening closed low at 500 mb near the southern tip of Nevada.* In the 1 December 2011 and 6 January 1997 events, the closed low at 500 mb was 546-552 dam. This pattern sets up strong north to NNE flow at the mid-levels over LA County.
3) *Strong synoptic-scale subsidence due to CAA on the western flank of the 500 mb low over LA County.*

4) *A strong east-west oriented surface high pressure system, setting up a strong north-south surface pressure gradient over southern California.* In the 6 January 1997 and 1 December 2011 events, the surface high was about 1036 mb and 1044 mb, respectively. LAX-BFL seems to do a better job of predicting the extreme events than LAX-SFO, likely because it focuses more on the surface pressure gradient over LA County. It appears that extreme events are more likely when LAX-BFL is -6 mb or stronger.

Less extreme events that still produce at least some wind damage may occur when the above conditions do not coincide or when one or more of the above is absent.

There are a number of other considerations regarding the likelihood of damaging winds for the foothill and valley areas south of the SGM as well. Aside from whether or not conditions are favorable for downslope winds, the synoptic-scale subsidence associated with CAA is likely the next most important factor with regards to the timing of the damaging winds. In four of the five cases examined here, the damaging winds began around the onset time of the strongest synoptic-scale subsidence associated with the CAA. This subsidence may occur in the wake of a strong cold front, as was the case in the 1 December 2011 event. The 1 December 2011 event also illustrated the importance of the strength and direction of the winds below the height of the inversion in the upstream environment. Finally, the time of day can be an important factor, as downslope wind storms are more likely to occur at night.

Despite the progress made in this study regarding the understanding of damaging downslope winds in the SGV and eastern SFV, plenty of room remains for future work. As previously stated, the case studies presented here attempted to distinguish between extreme events like 1 December 2011, and damaging, but less significant events. It would also be beneficial to study null events; i.e., events that exhibited some or all above synoptic-scale conditions, but did not produce any wind damage. This could lead to a more complete understanding of downslope wind storms in this part of southern California. It may also be useful to examine similar events for some of the other east-west oriented mountain ranges in southern California, such as the San Bernardino Mountains.

While the above suggestions for future work could be beneficial, it would be difficult to gain quantitative results due to the limited number of available case studies. For this reason, the best way forward may be to focus on studying the ability of high resolution models to forecast such events. As seen in Figure 17, a 1.3-km version of the Weather Research and Forecasting (WRF) model made a seemingly accurate forecast of 10-m wind gusts at 0800 UTC 1 December 2011, which was during the middle of the event. The 20-hr forecast valid at this time indicated the potential for 50-65 kt gusts for areas immediately south of the SGM (Fig. 17), where the worst of the wind damage occurred. Although the results of this forecast are promising, many other events would have to be looked at using various model resolutions and configurations.

Acknowledgements. The author would like to thank everyone at LOX who reviewed this paper and provided feedback. In particular, this includes forecasters Curt Kaplan and David Bruno, along with the Science Operations Officer (SOO), John Dumas, and Meteorologist in Charge (MIC), Mark Jackson. The author would also like to give a special thanks to Mark Jackson for giving him the opportunity to present the results of some of this research at the American Meteorological Society's 16th Conference on Mountain Meteorology in San Diego, CA in August 2014.

REFERENCES

Bluestein, H. B., 1992: *Principles of Kinematics and Dynamics*. Vol. I. *Synoptic-Dynamic Meteorology in Midlatitudes*. Oxford University Press, 431 pp.

COMET® Program, cited 2014: Mountain Waves and Downslope Winds. [Available online at http://www.meted.ucar.edu/mesoprim/mtnwave/print.htm.]

Durran, D.R., and J.B. Klemp, 1983: A compressible model for the simulation of moist mountain waves. Monthly Weather Review, **111**, 2341-2361.

Durran, D.R., 1990: Mountain waves and downslope winds. AMS Monograph Atmospheric Processes over Complex Terrain, Chap. 4, (in print).

Galarneau, T., cited 2014: Real-Time QG Diagnostics. [Available online at http://www2.mmm.ucar.edu/people/tomjr/files/realtime/diagnostics.html.]

Kaplan, C., and R. Thompson 2009: The Palmdale Wave: An example of mountain wave activity on the lee side of the San Gabriel Mountains. Western Regional Technical Attach Lite No. 09-05.

Raphael, M.N., 2003: The Santa Ana Winds of California. *Earth Interactions*, **7**, 8-20.

Ryan, G., 1996: Downslope Winds of Santa Barbara County, California. Western Region Technical Memorandum NWS WR-240, National Weather Service Western Region, Oxnard, California.

The City of Rosemead, cited 2014: Windstorm Hazards in the City of Rosemead. [Available online at http://www.cityofrosemead.org/Modules/ShowDocument.aspx?documentid=816.]

Whiteman, C.D., and J.G. Whiteman, 1974: A historical climatology of damaging downslope windstorms at Boulder, Colorado. *NOAA Technical Report ERL 336-APCL 35.* Available from the Superintendent of Documents, U.S. Government Printing Office, Washington, D.C.

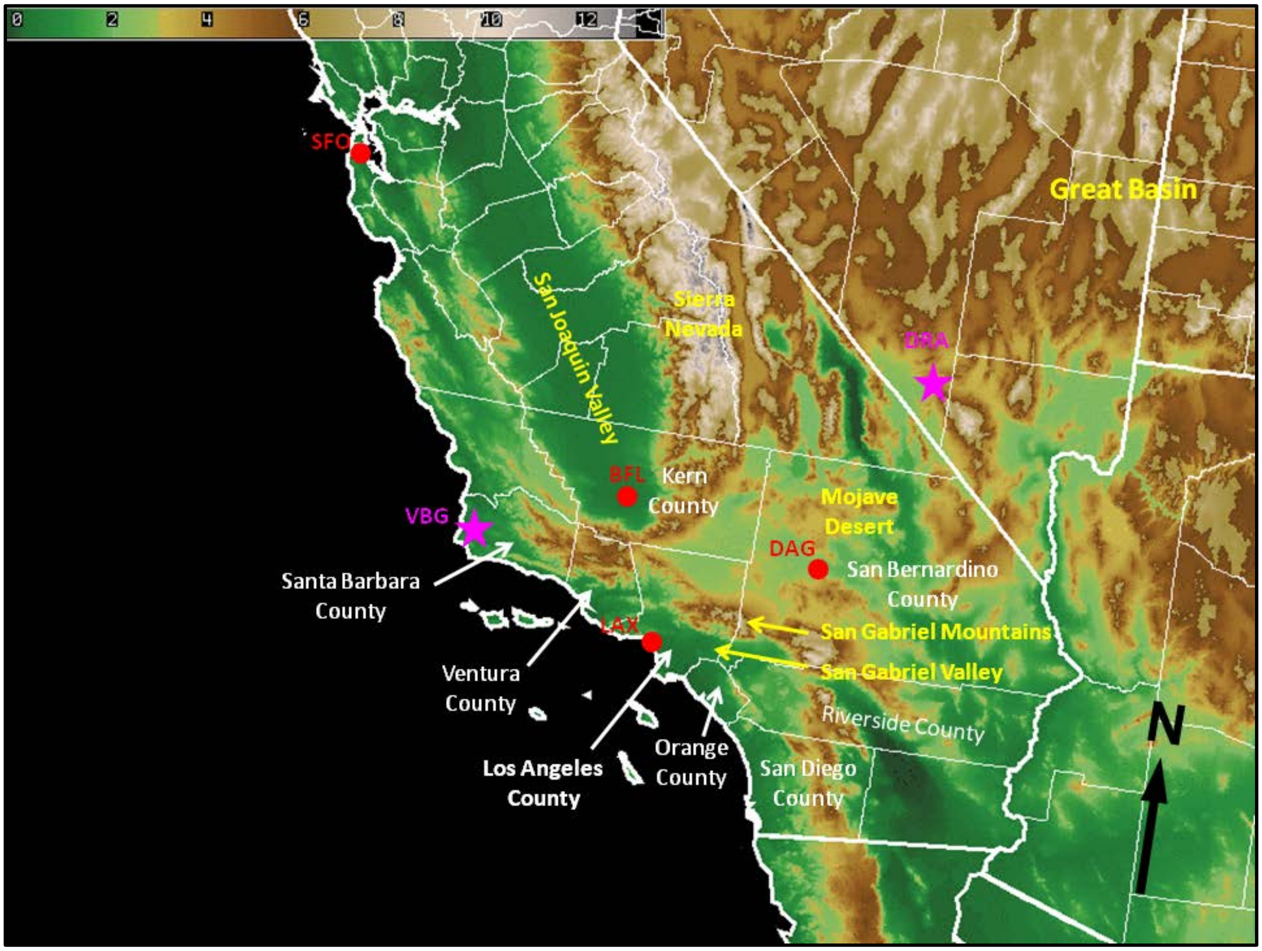

Fig. 1. Geographical overview of the region, including the locations of surface observation sites at San Francisco International Airport (SFO), Bakersfield (BFL), Daggett (DAG), and Los Angeles International Airport (LAX), along with Vandenberg Air Force Base (VBG) and Desert Rock (DRA) upper air sites. Thick white lines are state and country borders and thin white lines are county borders.

Fig. 2. Geographical overview of Los Angeles County including the locations of the Saugus RAWS sensor (SAUC1), Van Nuys Airport (VNY), Bob Hope Airport (BUR) in Burbank, the Santa Fe Dam RAWS sensor (STFC1), and Los Angeles International Airport (LAX). Thick black lines represent the county borders and the thin black lines are the zone forecast boundaries for NWS Los Angeles/Oxnard. The orange shaded area south the San Gabriel Mountains is the region for which a climatology of damaging wind events was constructed using National Climatic Data Center (NCDC) Storm Data and the NCDC Online Storm Events Database (see text). Background map is courtesy of www.maphill.com.

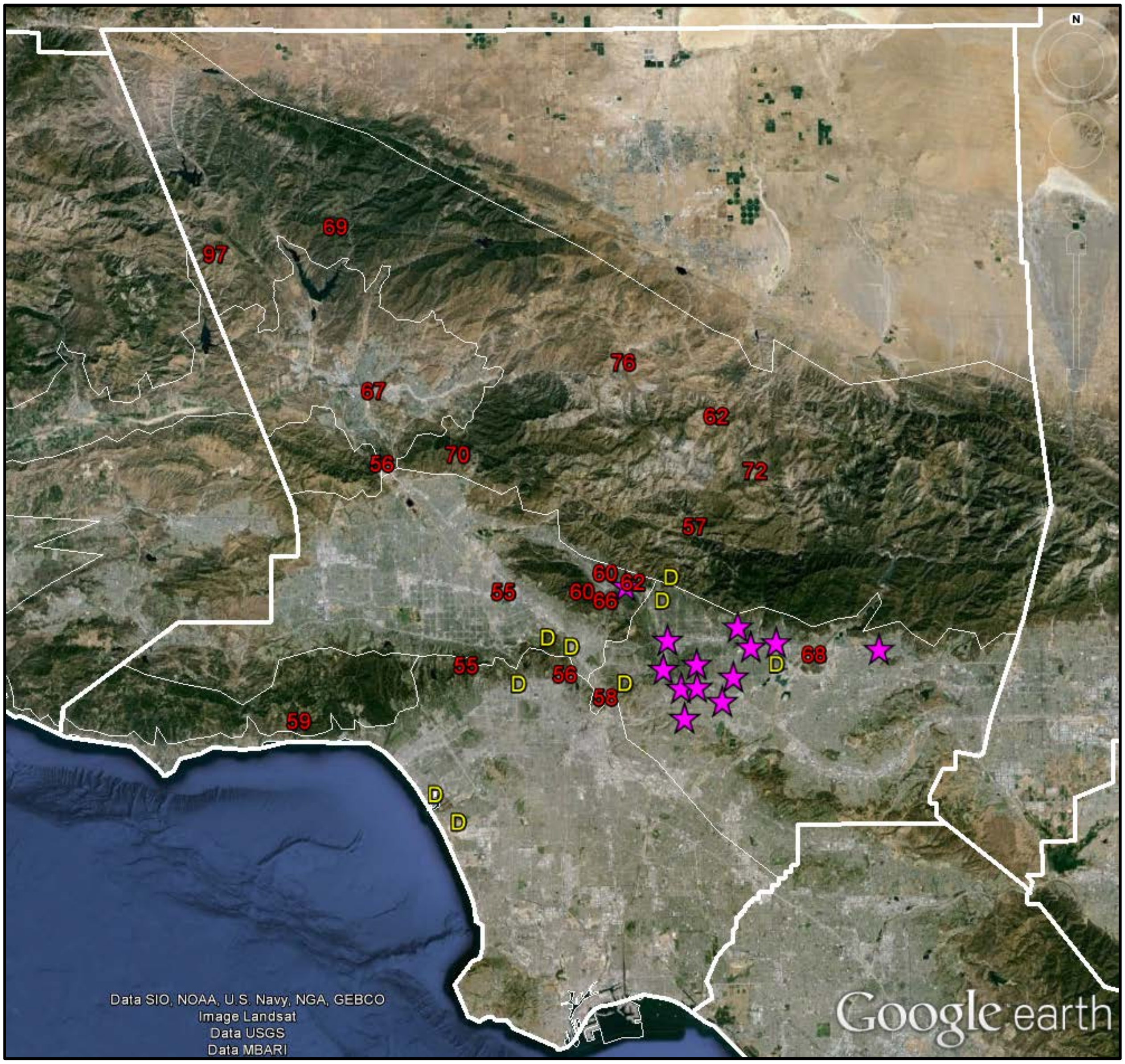

Fig. 3. Overview of the maximum wind gusts and wind damage from 0000 UTC 1 December 2011 through 0000 UTC 2 December 2011. Wind damage in the foothill and valley areas south of the San Gabriel mountains occurred mostly from 0600 – 1200 UTC 1 December 2011. The red numbers are measured gusts (mph) from Local Storm Reports (LSR) issued by NWS Los Angeles/Oxnard. Each yellow "D" represents a report of wind damage, also from LSRs issued by NWS Los Angeles/Oxnard. Pink stars indicate the cities and communities that declared a Proclamation of Local Emergency due to wind damage.

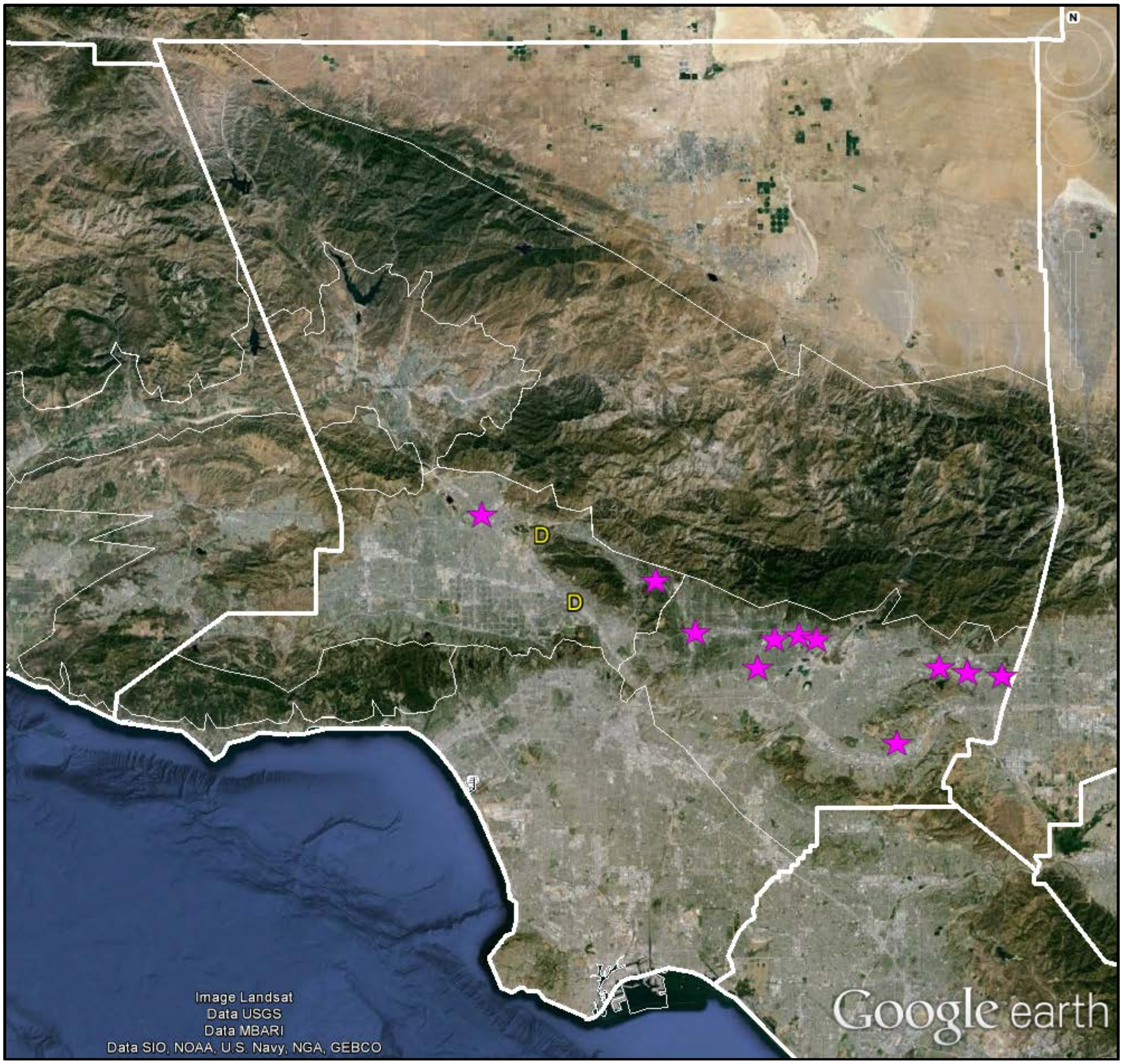

Fig. 4. Map showing cities with wind damage that were mentioned in the NCDC storm summary for the 6 January 1997 event. The pink stars indicate cities that declared a Local State of Emergency due to wind damage and each yellow “D” represents an additional city that was mentioned in the storm summary.

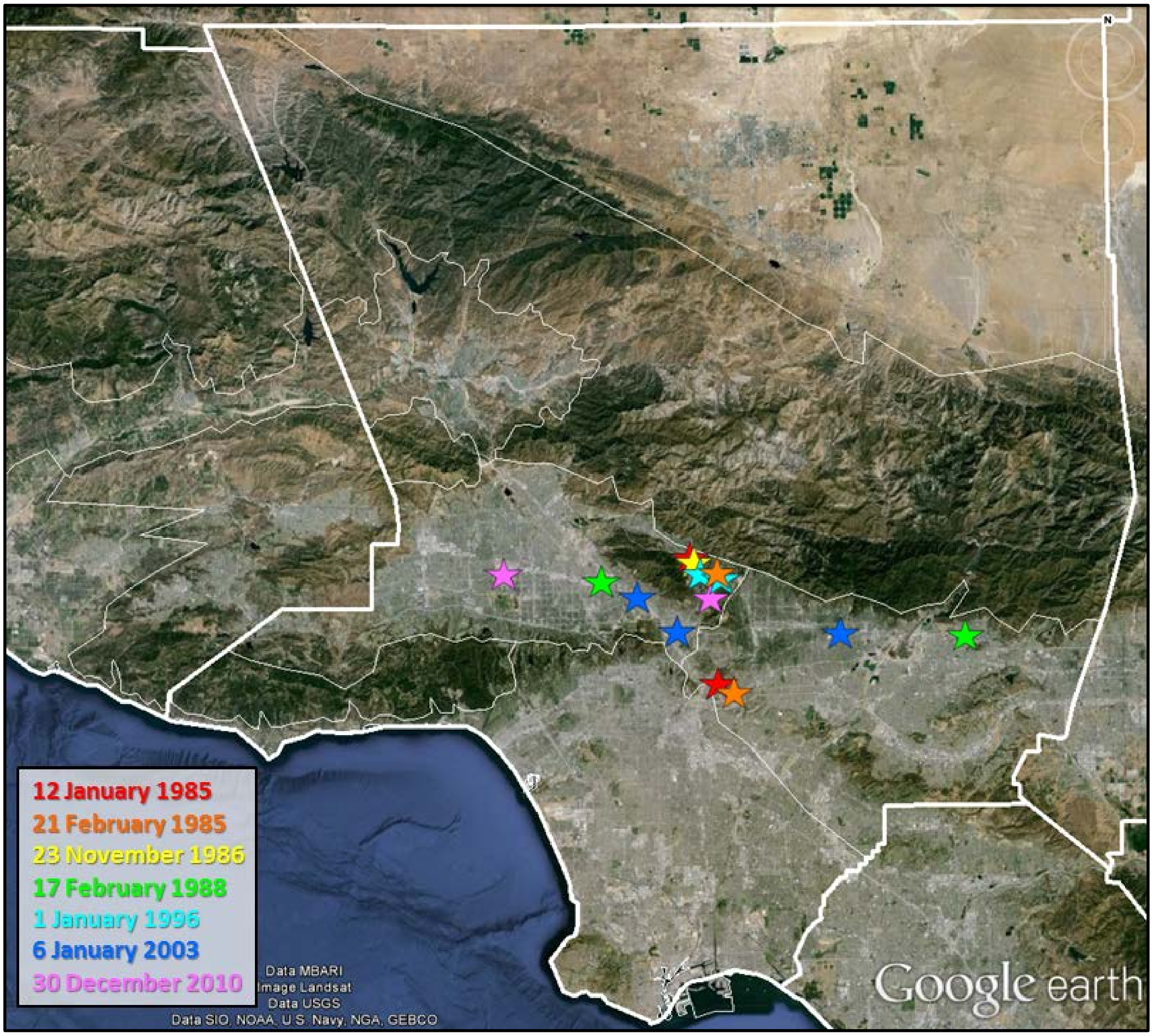

Fig. 5. Map showing locations with wind damage for the seven remaining events in the 35-year climatology (i.e. events other than 6 January 1997 and 1 December 2011). The colored stars represent cities that were mentioned in the NCDC storm summaries, with the exception of 6 January 2003 (see main text). Each event has its own color according to the legend in the lower left.

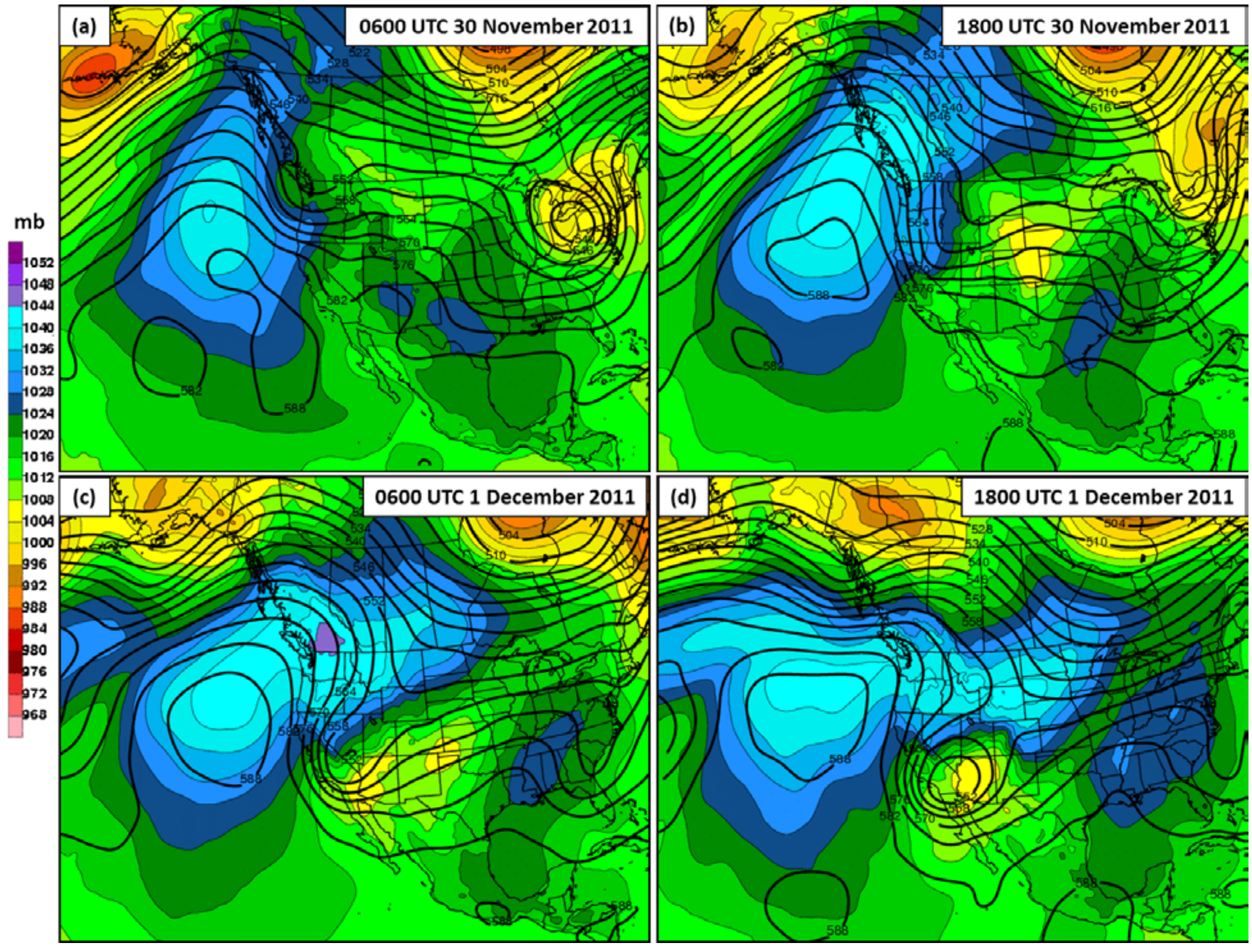

Fig. 6. 500 mb heights (thick black contours, dam) and mean sea level pressure (shaded and contoured in thin black contours, mb) at a) 0600 UTC 30 November 2011, b) 1800 UTC 30 November 2011, c) 0600 UTC 1 December 2011, and d) 1800 UTC 1 December 2011. Data source is the North American Regional Reanalysis (NARR).

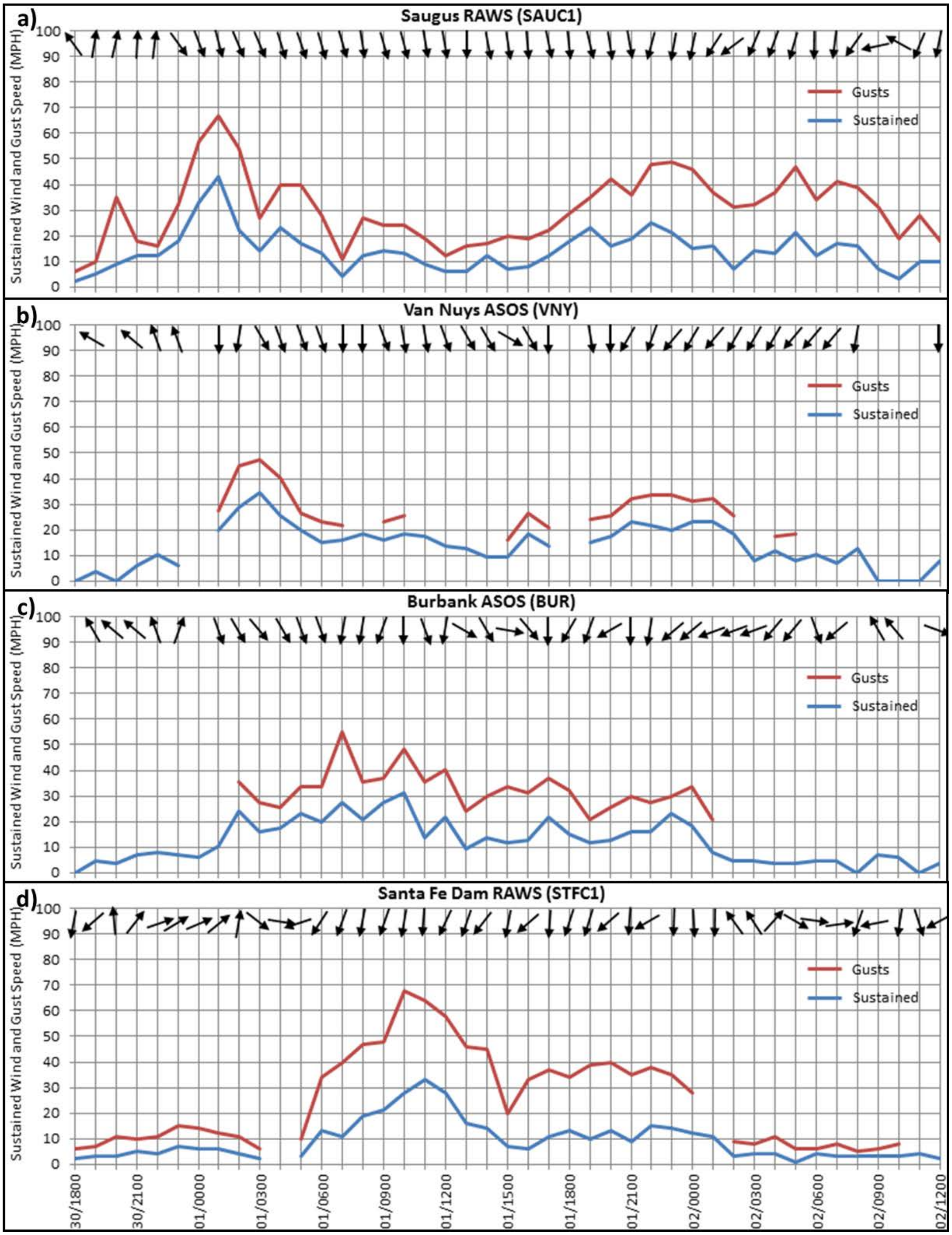

Fig. 7. Sustained wind speeds (blue) and gusts (red) in MPH for the a) Saugus RAWS (SAUC1), b) Van Nuys ASOS (VNY), c) Burbank ASOS (BUR), and d) Santa Fe Dam RAWS (STFC1) from 1800 UTC 30 November 2011 through 1200 UTC 2 December 2011. Arrows indicate the prevailing wind direction. See Figure 2 for locations of these sites.

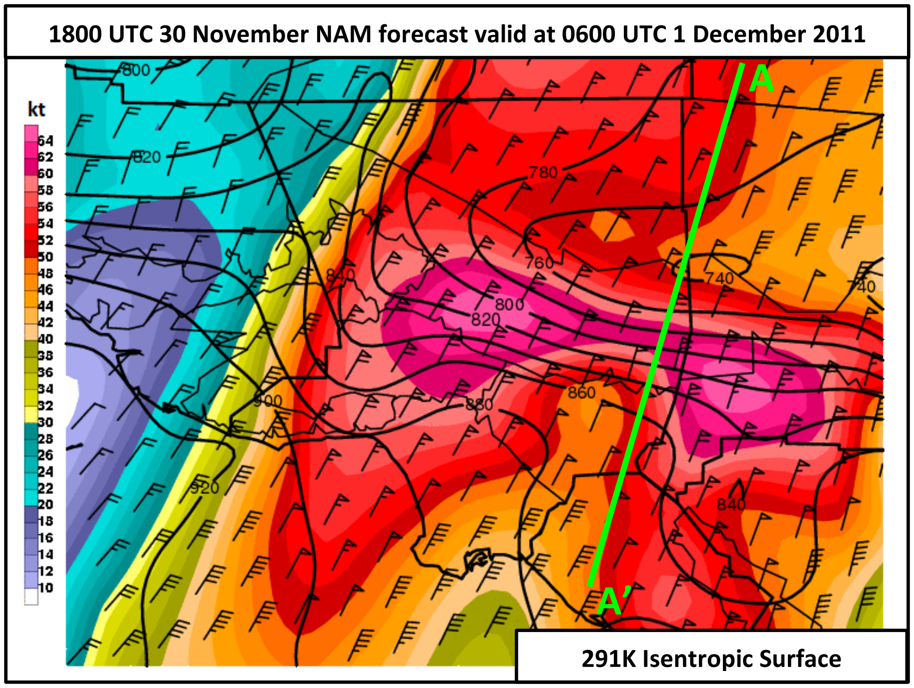

Fig. 8. Isentropic analysis of vector winds (barbs, kt), vector winds (shaded, kt), and pressure (black contours, mb) on the 291K potential temperature surface from the 1800 UTC 30 November 2011 12-hr NAM forecast valid at 0600 UTC 1 December 2011.

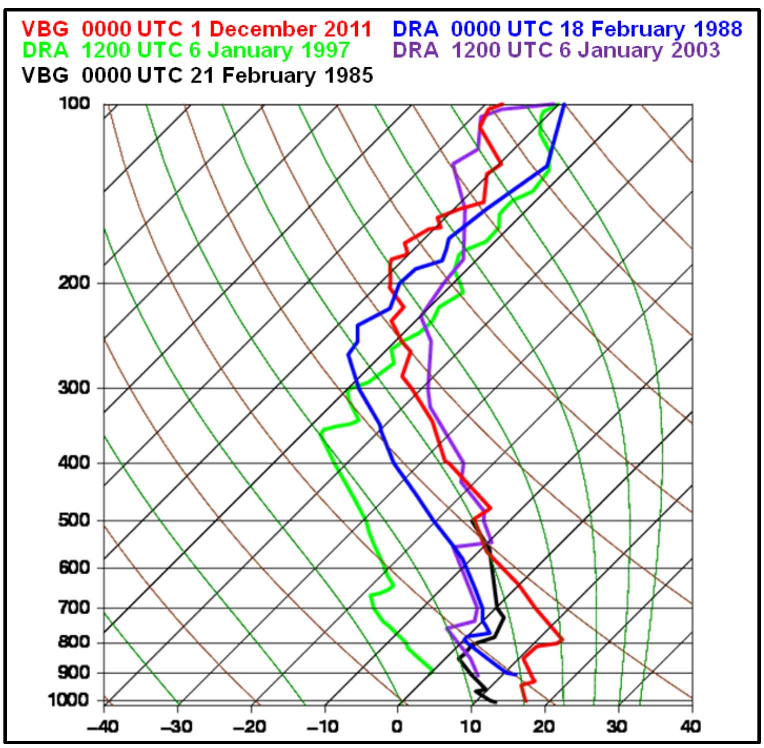

Fig. 9. Temperature profiles plotted on a skew-T diagram for 0000 UTC 1 December 2011 at VBG (red), 1200 UTC 6 January 1997 at DRA (green), 0000 UTC 21 February 1985 at VBG (black), 0000 UTC 18 February 1988 at DRA (blue), and 1200 UTC 6 January 2003 at DRA (purple). See Figure 1 for the locations of VBG and DRA. Data source: https://mesonet.agron.iastate.edu/archive/

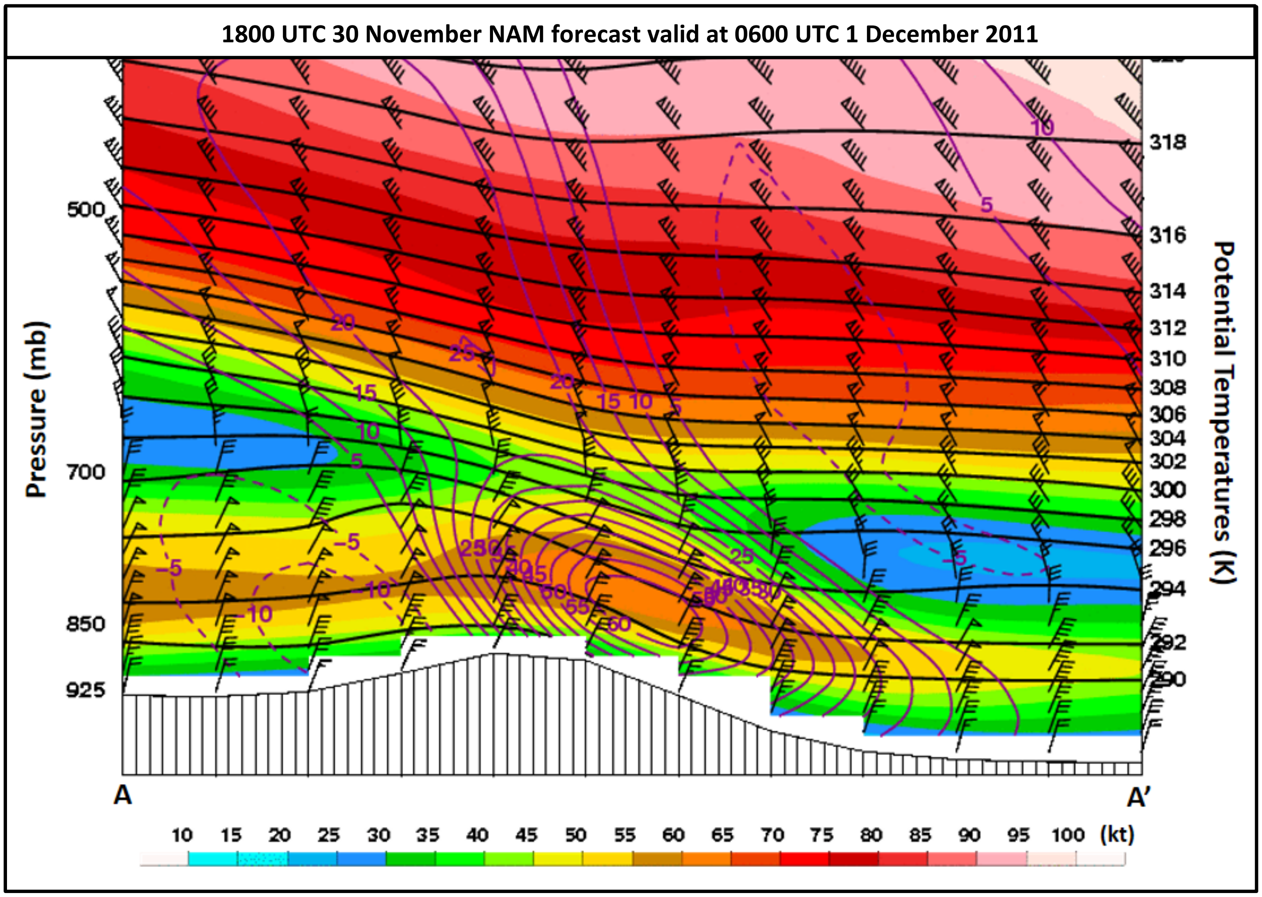

Fig. 10. Cross section of vector winds (barbs, kt), wind speeds (shaded, kt), potential temperature (solid black contours, K), omega (dash and solid purple contours, μb/s). Regions of descent (ascent) are plotted in solid (dashed) purple contours every 5 μb/s. Data plotted is from the 1800 UTC 30 November 2011 12-hr NAM forecast valid at 0600 UTC 1 December 2011. Line A-A' is shown in Figure 8.

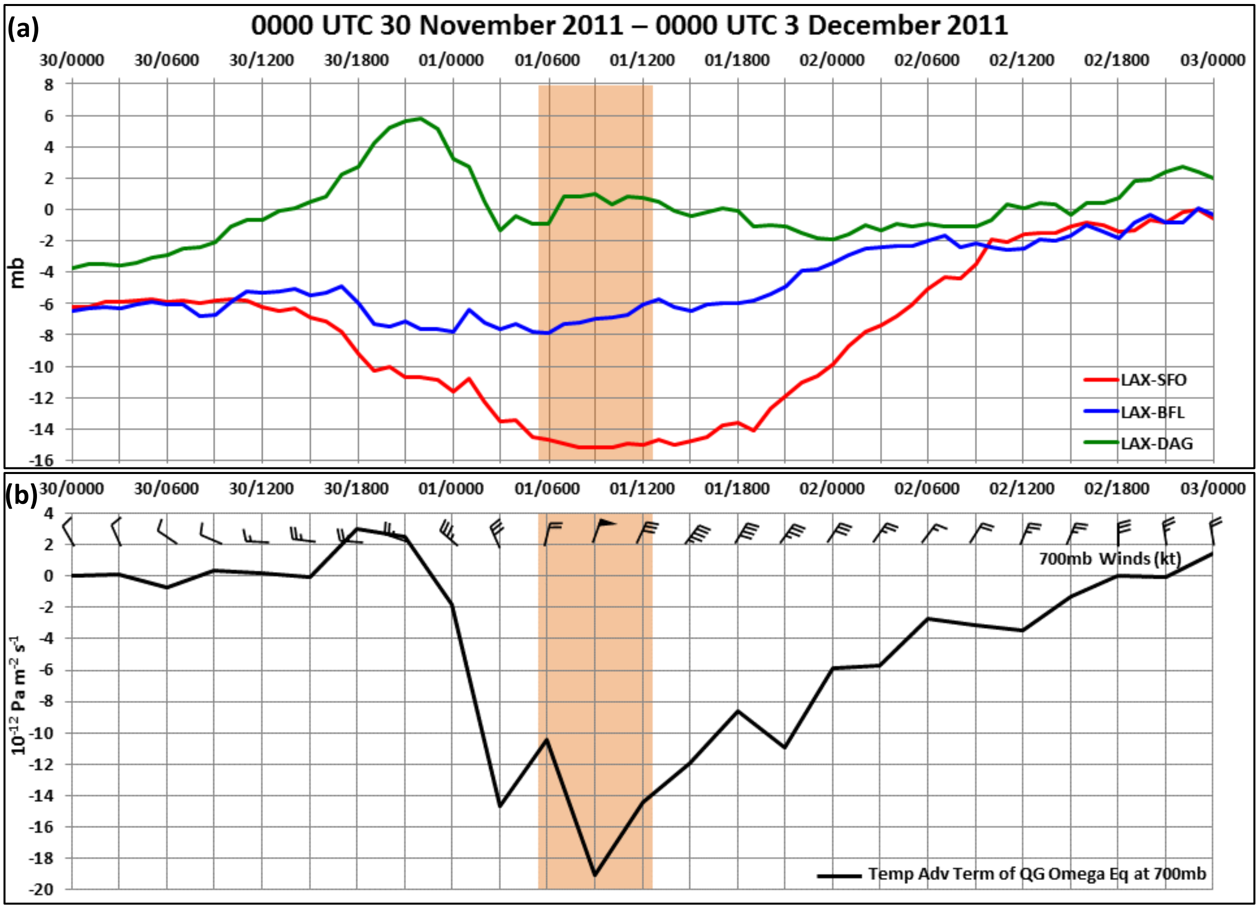

Fig. 11. Panel (a) displays a time series of mean sea level pressure differences from METAR observations between Los Angeles International Airport and San Francisco International Airport (red, mb), Los Angeles International Airport and Bakersfield (blue, mb), and Los Angeles International Airport and Daggett (green, mb). Panel (b) displays a time series of 700 mb winds (wind barbs, kt) and the temperature advection term of the quasi-geostrophic (QG) omega equation evaluated at 700 mb (black, 10^{-12} Pa m^{-2} s^{-1}). This is Term B on the right hand side of equation 5.6.11 from Bluestein (1992, page 329), which is the horizontal Laplacian of temperature advection. The Term B values shown here indicate forcing for vertical motion rather than actual omega values. Negative (positive) values are associated with downward (upward) vertical motion. Values in panel (b) are for a grid point over the San Gabriel Mountains and are calculated from the North American Regional Reanalysis (NARR). The tan shaded region in (a) and (b) indicates the approximate period when the damaging winds occurred in the foothill and valley areas south of the San Gabriel Mountains. The time series are from 0000 UTC 30 November 2011 through 0000 UTC 3 December 2011.

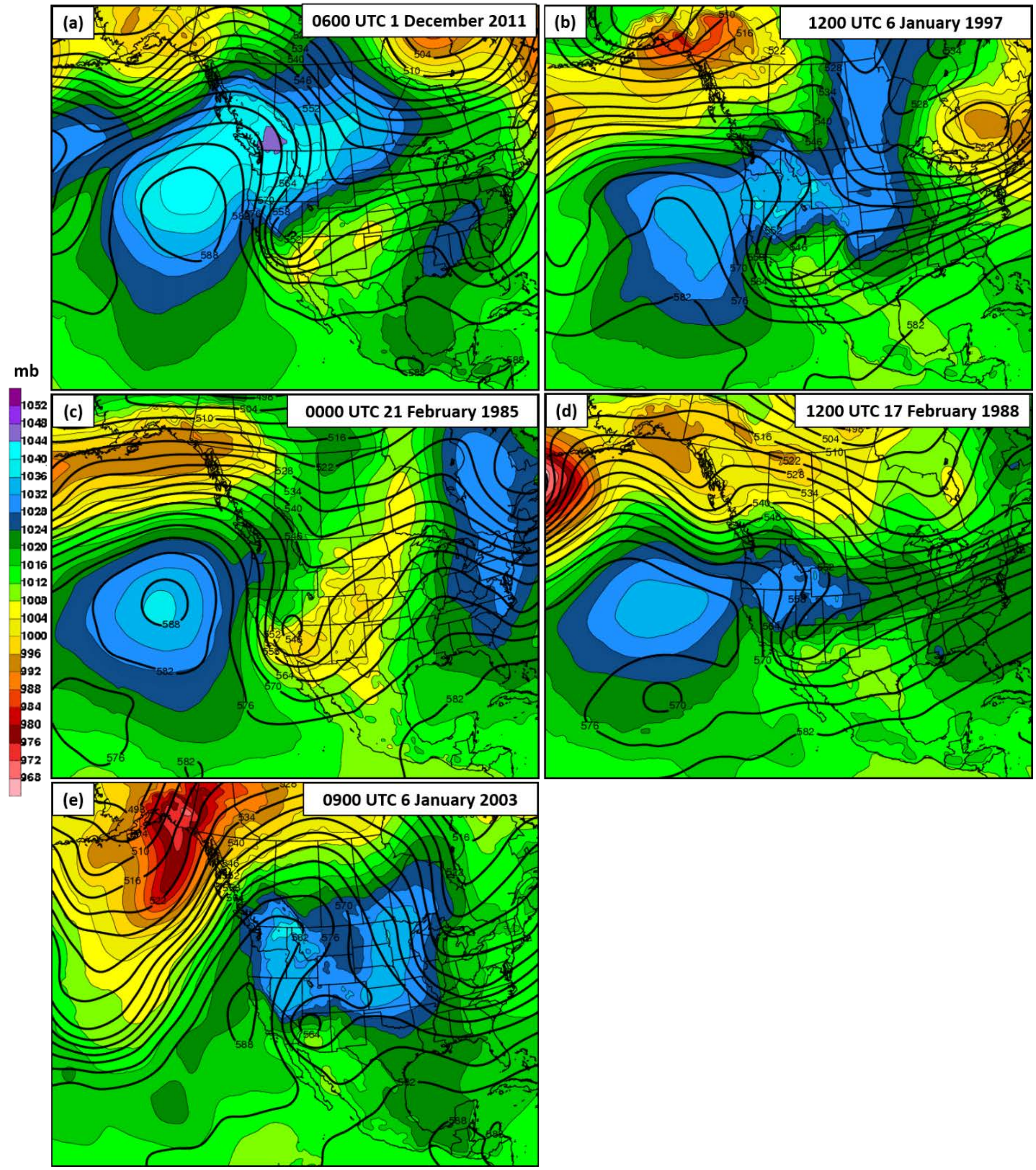

Fig. 12. Same as Figure 6 except for a) 0600 UTC 1 December 2011 b) 1200 UTC 6 January 1997, c) 0000 UTC 21 February 1985, d) 1200 UTC 17 February 1988, and e) 0900 UTC 6 January 2003. Times shown are the approximate start time of the damaging winds in the foothill and valley areas south of the San Gabriel Mountains for each event.

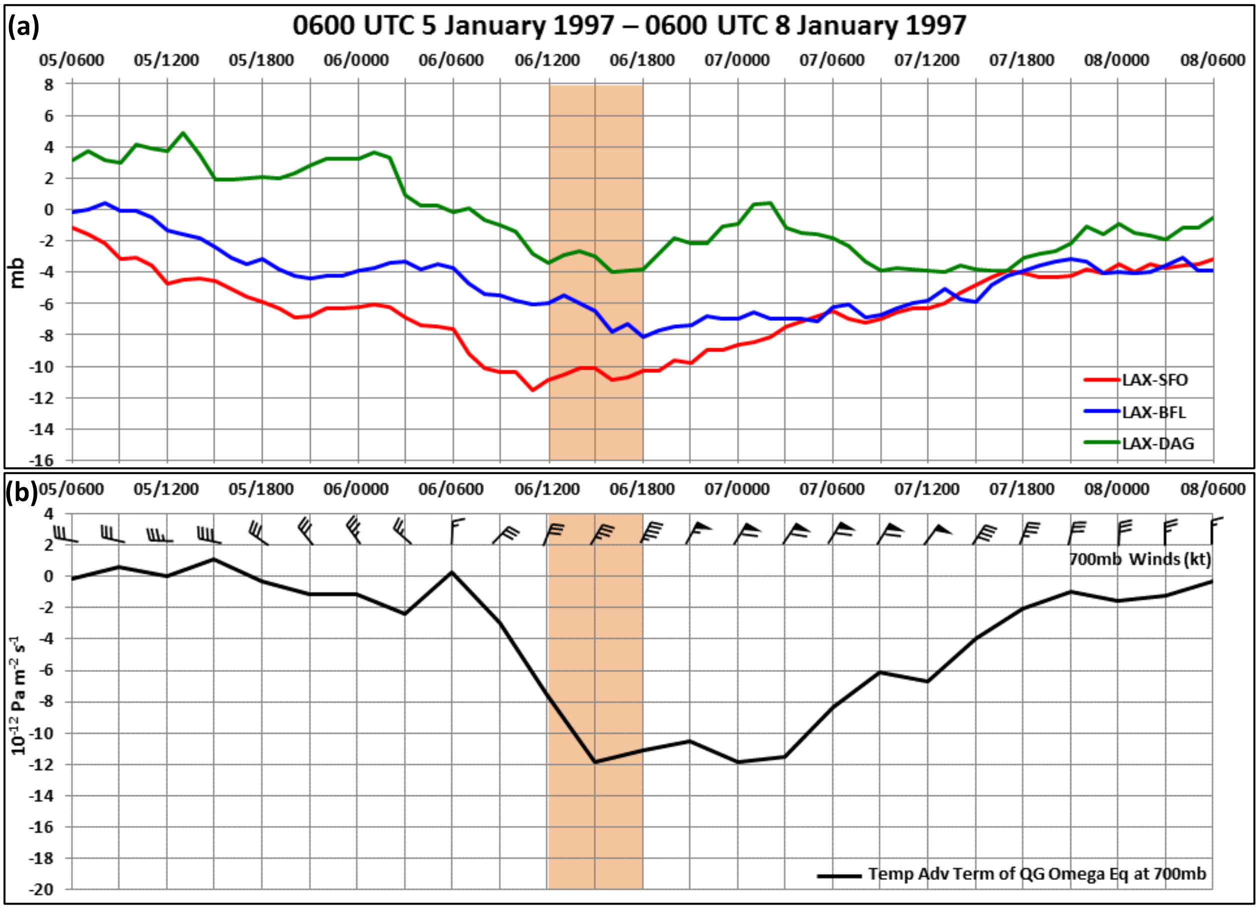

Fig. 13. Same as Figure 11, except for 0600 UTC 5 January 1997 through 0600 UTC 8 January 1997.

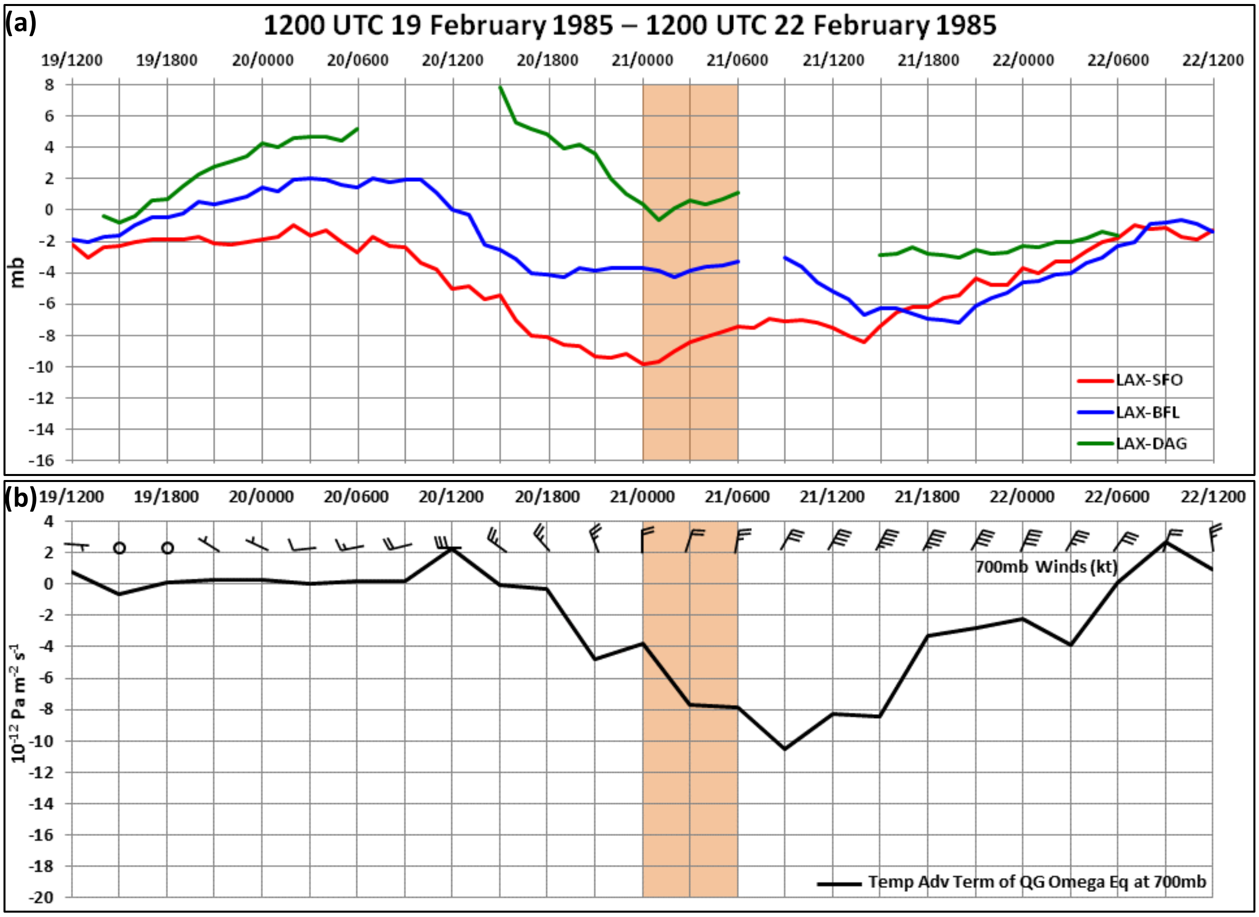

Fig. 14. Same as Figure 11, except for 1200 UTC 19 February 1985 through 1200 UTC 22 February 1985.

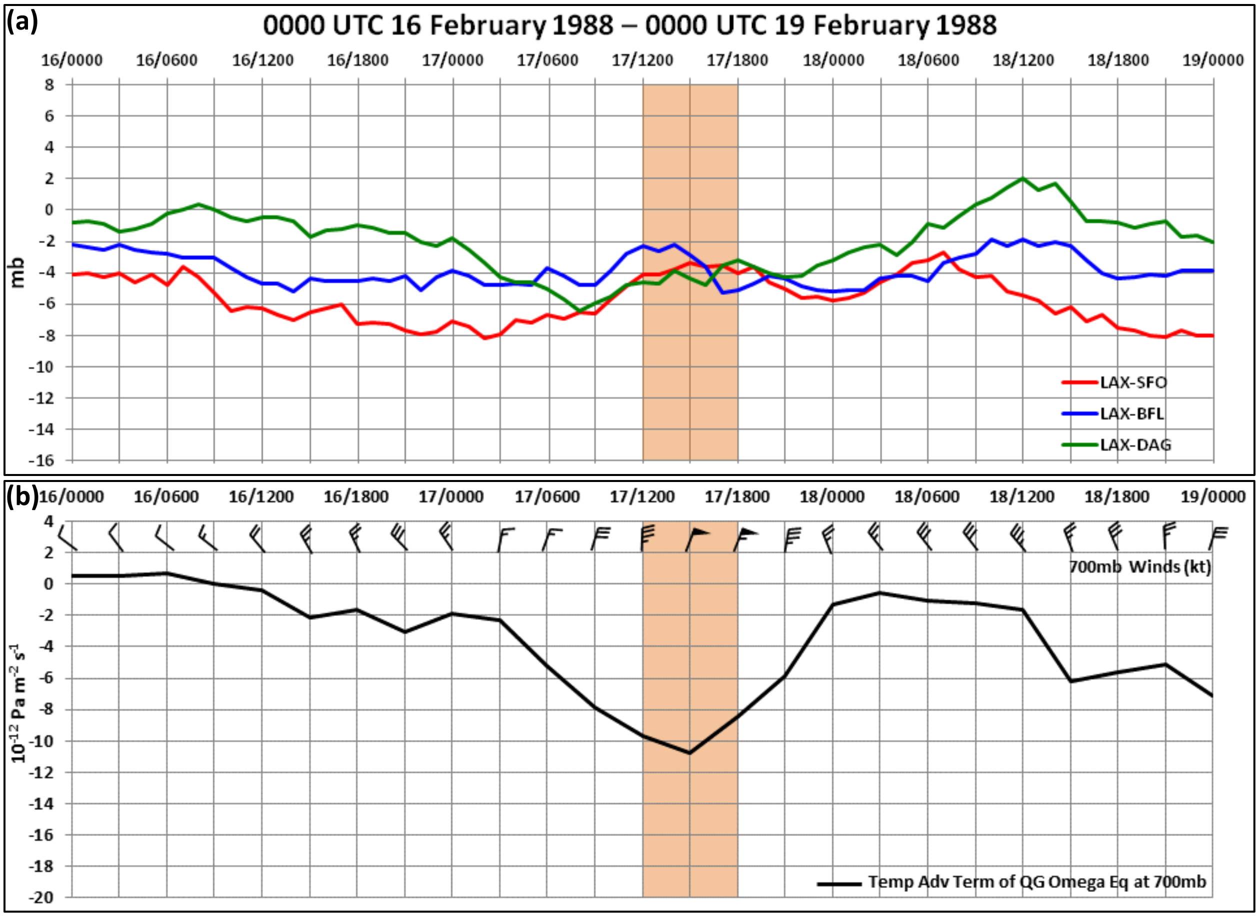

Fig. 15. Same as Figure 11, except for 0000 UTC 16 January 1988 through 0000 UTC 19 February 1988.

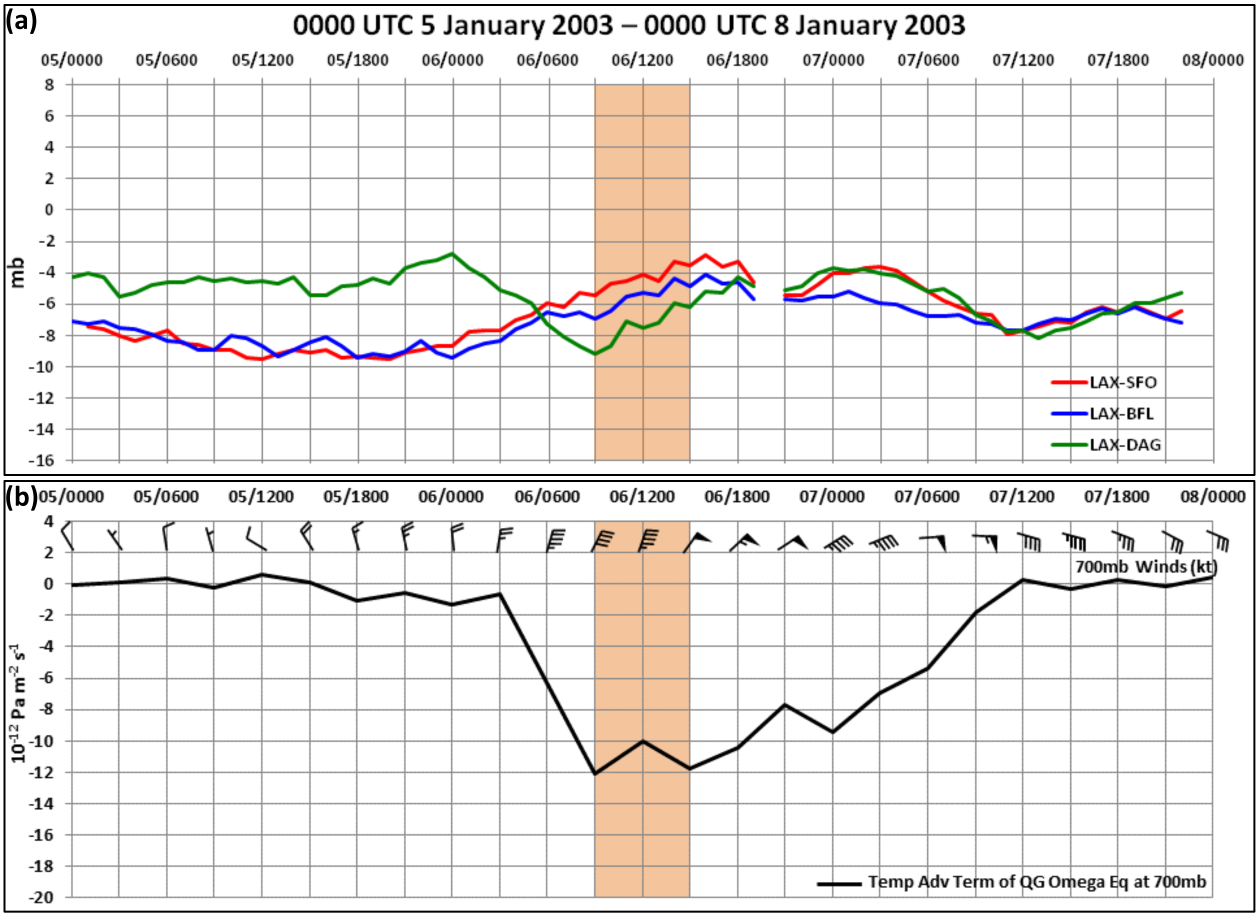

Fig. 16. Same as Figure 11, except for 0000 UTC 5 January 2003 through 0000 UTC 8 January 2003.

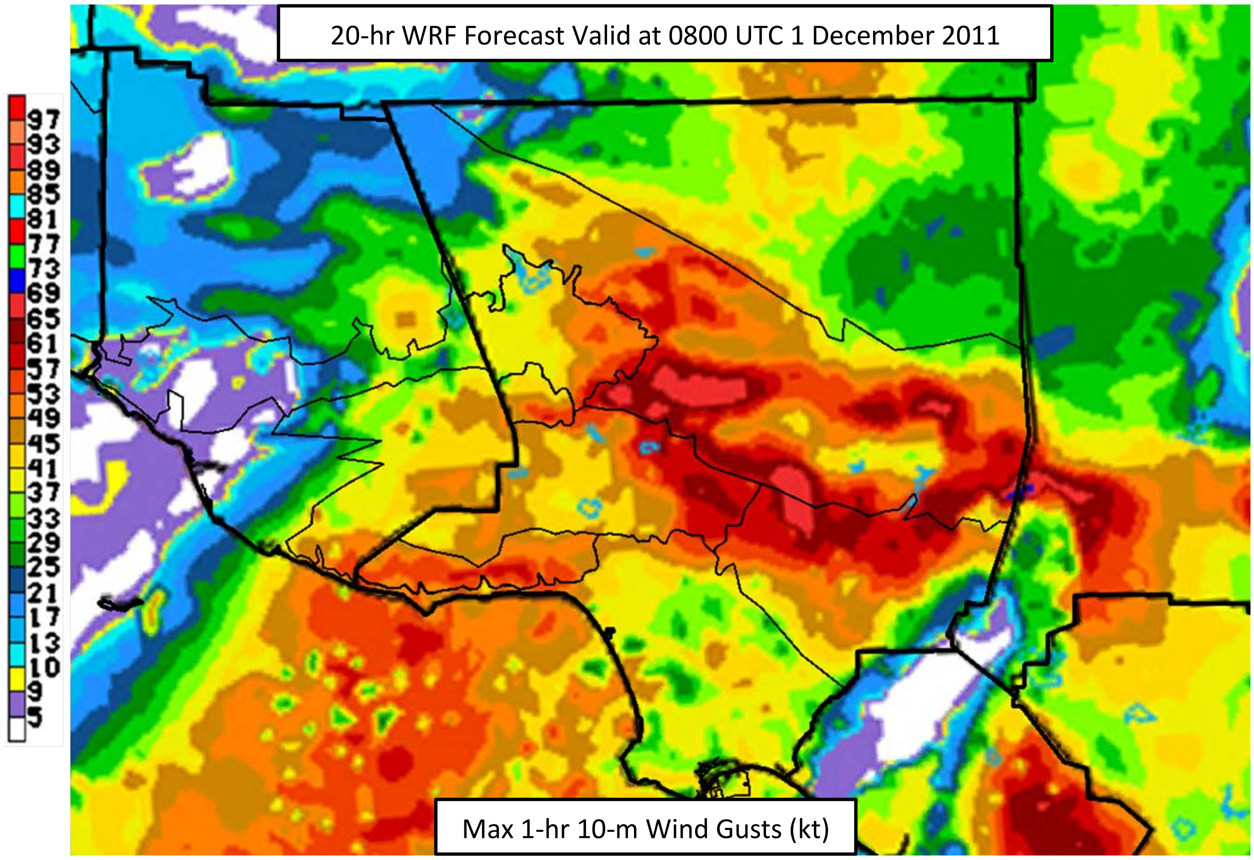

Fig. 17. A 20-hr forecast of the maximum 10-m wind gusts (kt) for the 1-hr period ending at 0800 UTC 1 December 2011. Forecast was made by a nested 1.3-km Weather Research and Forecasting (WRF) model ran at the Environmental Prediction Center (EPC). The model was initialized at 1200 UTC 30 November 2011 by the Storm Prediction Center (SPC) in support of fire weather operations at NWS Los Angeles/Oxnard.